

ROTOR DYNAMIC LOADS CHARACTERISTIC ANALYSIS WITH BLADE TIP TWIST DISTRIBUTION

YU Zhihao, HUANG jian, JIANG Qihuang, FAN Feng, HUANG Shuilin

National Key Laboratory of Helicopter Aeromechanics, China Helicopter Research Design Institute, China, Jingdezhen

Abstract

A method for computing aeroelastic loads on rotor blades was employed, and the issue of rotor dynamics in high-speed forward flight was analyzed with the aim of addressing the problem of dynamic load variation caused by different tip twist distributions in conventional helicopters. A slender and flexible rotor blade was utilized to construct a multi-body dynamics model using the Hamilton principle and middle deformation beam theory. The aerodynamic model was developed based on a dual free wake model to account for negative lift at the blade tip. Finally, the validity of the computing method was confirmed through its application in analyzing load characteristics influenced by blade tip twist design. The analysis of the BO105 rotor revealed that employing a larger linear negative twist would enhance rotor efficiency at lower flight speeds and reduce impaction in dynamic loads. However, at medium or higher speeds, the expansion of the negative lift area at the blade tip would lead to increased rotor dynamic loads. Conversely, implementing a positive twist and sweep design at the blade tip would decrease rotor dynamic loads. These findings were further validated by wind tunnel testing of a 4m diameter model rotor.

Key words: helicopter, rotor, dynamic load, twist distribution

1 Introduction

The rotor system is a fundamental component of helicopters and serves as the primary source of vibration. During high-speed forward flight, the rotor experiences forward blade shock waves and backward blade stall, both contributing to increased vibration levels[1]. The development of low-vibration rotor systems represents an innovative direction for helicopter technology. Full-scale wind tunnel testing of the UH-60A[2] has revealed that in high Mach number conditions, the aerodynamic center of the rotor blade moves towards the trailing edge, resulting in a significant offset aerodynamic

moment and noticeable elastic torsion motion. Attention should be given to negative lift and reverse flow phenomena. Recent research[3] on the complex three-dimensional design of rotor blades has demonstrated that dynamic loads increase as a result of blade vortex interaction. An optimal distribution of twist angle in the blade can enhance aerodynamic performance while effectively reducing vibration loads. However, excessive distribution of negative twist angle leads to a sharp increase in high-level vibration loads. The research conducted by the Eli[4,5] team demonstrated that appropriately augmenting negative blade torsion could enhance rotor hover efficiency. However, excessive negative torsion may lead to an escalation in dynamic load levels during forward flight. Vincenzo's research[6] has demonstrated that a smaller negative twist angle in the blade tip would lead to improved aerodynamic stability and reduced pitch link loads. Pavel[7] proved that through the implementation of a well-designed blade torsional distribution and structural configuration, as well as the utilization of flaptorsional inertia coupling and aerodynamic structure coupling, it is possible to effectively mitigate blade root shear and bending moment, thereby achieving a reduction in load. Currently, the majority of research teams focus on utilizing materials such as piezoelectric fibers [8,9], memory alloys [10,11], and other similar materials to achieve active variable torsion in blade applications. However, most of these studies are centered around rotor performance and noise.

This paper primarily focuses on the impact of blade tip torsion distribution on rotor vibration loads in a conventional configuration helicopter. A computational model for rotor aeroelastic loads was utilized, and the rotor multi-body dynamics model was constructed using the Hamilton principle and middle deformation beam theory. The aerodynamic model was developed based on a dual free wake model to capture negative lift at the blade tip. Furthermore, an analysis of rotor dynamics issues in high-speed forward flight was conducted with the aim of addressing variations in rotor dynamic loads resulting from different tip twist distribution designs in conventional helicopters.

2 Numerical computing method

The rotor system comprises numerous components, including blades, flap/edge hinges, pitch mechanisms, dampers, pitch links, and more. It represents a classic multi-body system with rigid and spring coupling. The rotor dynamic method employed in this study is based on the principles of multi-body dynamics, with the spatial position of the rotor being established using a floating coordinate system. Furthermore, the assembly of components is achieved through constraint relationships.

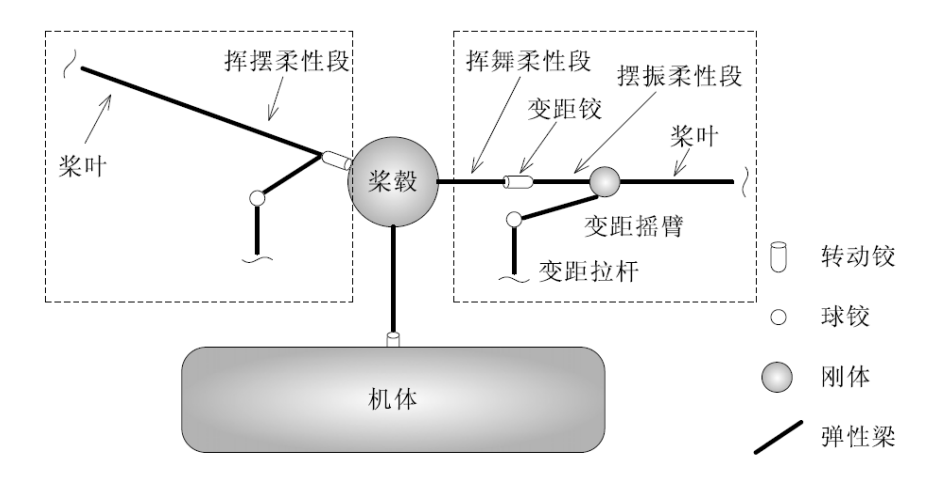


Fig 1 Rotor system

In the blade component, the Hamilton principle and the middle deformation beam theory were employed. The system strain energy was formulated based on Green's strain relationship and isotropic hypothesis. In the equation, Q represent the constitutive equations, ϵ represent strain matrix, \mathbf{A} represent blade cross section area. The right end of equation were generalized force, and \mathbf{F}_{U} represent nonlinear generalized force, \mathbf{q}_{D} represent generalized degree of freedom matrix.

$$\delta \mathbf{U} = \iint (\delta \mathbf{\varepsilon}^T \mathbf{Q} \mathbf{\varepsilon}) dA dx = \delta \mathbf{q}_b^T \mathbf{F}_U$$

The system kinetic energy were built as follows, the rigid and elastic motion were described in floating coordinate system, which contains flap/lag/torsion motion. The left end of equation, system mass matrix came from kinetic energy, \mathbf{M}_b represent mass matrix of blade motion, \mathbf{F}_M represent nonlinear generalized force from blade flap/lag/torsion motion. The virtual work were built as follows, the blade external load came from aerodynamic force. \mathbf{F}_A represent nonlinear generalized aerodynamic force.

$$\delta \mathbf{W} = \delta \mathbf{q}_b^T \mathbf{F}_A$$

According to system strain energy, kinetic energy and virtual work, the systemdynamic equations were built as follows, \mathbf{G}_b represent the coefficient matrix of nonlinear generalized aerodynamic force, \mathbf{f}_c represent concentrated loads.

$$\mathbf{M}_{b}\ddot{\mathbf{q}}_{b} - \ddot{\mathbf{G}}_{b}\mathbf{f}_{c} = \mathbf{F}_{A} - \mathbf{F}_{M} - \mathbf{F}_{U}$$

The aerodynamic loads on rotor blades are primarily determined by the lift line theory, and the induced velocity of the rotor is calculated using a free wake model. In high-speed flight, a dual free wake model is employed to accurately capture negative lift at the blade tip and rotor interaction. The W-L lift surface model was used in blade section aerodynamic force, as follows. ρ represent air density, U represent flow velocity, Γ represent bound vortex circulation.

$$L = \rho U \Gamma$$

The circulation of trailing vortex was the subtract of adjacent circulation of blade element. $\Gamma_{n,j}$ respresent the jth trailing vortex circulation, $\Gamma_{b,j}$ respresent the jth bound vortex circulation, N_s respresent numbers of blade element.

$$\Gamma_{n,j+1} = \Gamma_{b,j} - \Gamma_{b,j+1}, j = 1,...,N_s$$

In high-speed flight, the generation of negative lift at the advancing blade tip has been demonstrated by some research[] to result in strong blade vortex interaction and serve as a source of vibration loads. Therefore, this paper employs the dual wake model to address these phenomena.

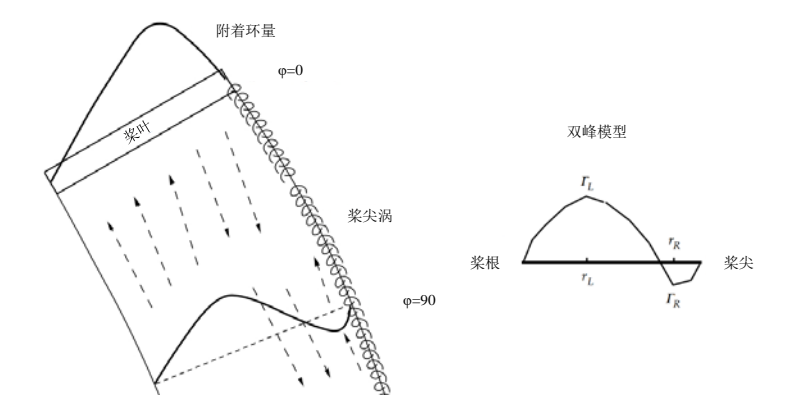


Fig 2 Rotor wake

The induced velocity cause by vortex was computed with Biov Savart law, as follows. **V** respresent the induced velocity, **I** respresent linear distance, **r** the space position vector.

$$d\mathbf{V} = \frac{\Gamma}{4\pi} \frac{d\mathbf{l} \times \mathbf{r}}{\left|\mathbf{r}\right|^3}$$

3 Validation

In order to validate the model presented in this paper, a rotor wind test (Fig 4) was conducted to verify the accuracy of vibration load calculations. The wind test involved two different rotors, with Tab 3 detailing the main parameters of the rotors and Fig 5 and 6 illustrating the aerodynamic shape and twist distribution of the blades. Specifically, for No.1 blade, there is zero twist distribution beyond 0.95 r, while for No.2 blade, there is a +15° twist distribution beyond 0.95 r. Both blades have a twist angle of 0° at the 0.7r section.

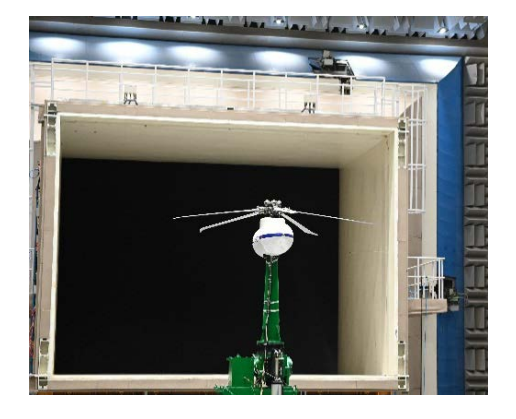


Fig 4 Wind tunnel test

Tab 1 Model rotor main parameter

| Parameter | Value | |
|---------------------|------------|--|
| Number of blade | 5 | |
| Blade radius /m | 2 | |
| Mean chord /m | 0.24 | |
| Rotor speed /rpm | 1055 | |
| Rotor configuration | Full hinge | |
| Taper ratio | 1:3 | |

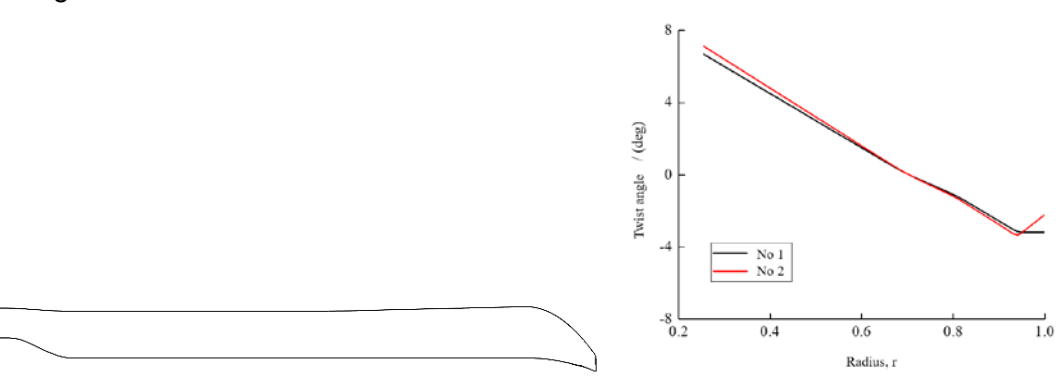
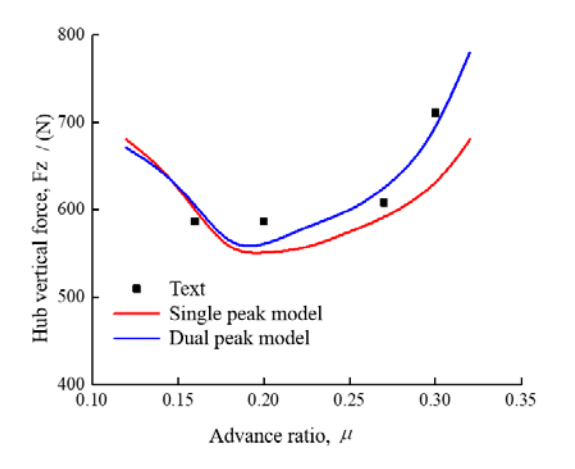


Fig 5 Blade aerodynamic shape

Fig 6 Blade twist distribution

Fig 7 are the 5th harmonic loads of hub vertical force result with test value, two wake model calculated value. Both of two different twist distribution rotor showed that hub vertical force would increase at high advance ratio. Two wake model showed that the equivalent ability in low advance ratio, due to there is no negative lift at blade tip in advancing side. But the calculated value of the dual wake model were more accurate with test value. The hub vertical force were lower, because No.2 blade is +15° twist distribution beyond 0.95 *r*, and the negative lift less than the other. The result indicated that the computing method in this paper have a good calculation accuracy in vibration loads.



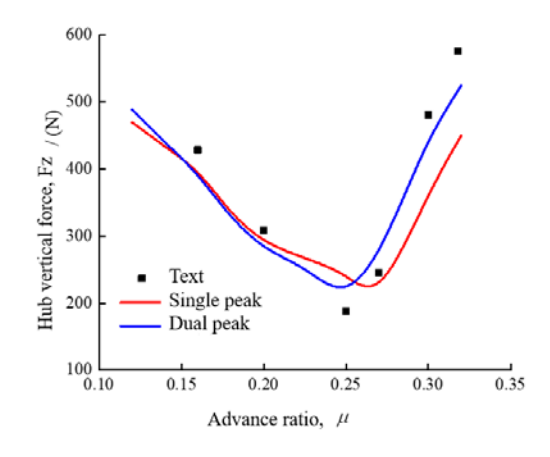


Fig 7 The 5th harmonic loads of hub vertical force

4 Analysis

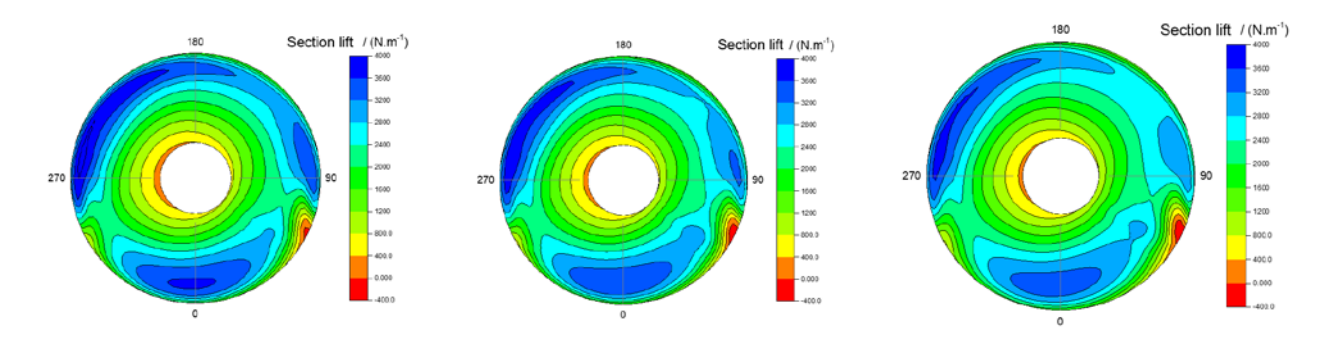
4.1 Bo105 rotor analysis

In order to analysis the effects of different negative torsion angles on the lift distribution of the rotor blade, blade tip response and vibration loads of root. The Bo105 rotor[13] was used in this part, and three linear twist distribution blade were assumed, focusing on the vibration loads characteristic in two fight speed (μ =0.1, 0.25).

Tab 2 BO105 rotor main parameter

| parameter | value |
|--------------------------|-------|
| Number of blade, N_b | 4 |
| Lock number, γ | 5.2 |
| Rotor solidity, σ | 0.07 |
| Rotor radius / m | 4.928 |
| Rotor speed / rpm | 425 |
| Blade chord / m | 0.055 |
| Blade twist / deg | 0 |

Fig 8 and Fig 9 were rotor lift disk in different flight speed and twist distribution. In low flight speed, the lift would concentrate at blade tip in, 0° , 90° and $180\sim270^{\circ}$ region. With the negative twist increase, the lift concentration in 0° , 90° region were alleviated at low speed flight (μ =0.1), and rotor lift peak value was decreased. The strong negative lift appeared in μ =0.25, and the negative twist would aggravated this phenomenon. The lift were concentrated at blade tip in, 0° , 180° region. Due to the negative lift at blade tip in 90° nearby region and lateral balance, the lift at blade tip in 180° nearby region were decreased.



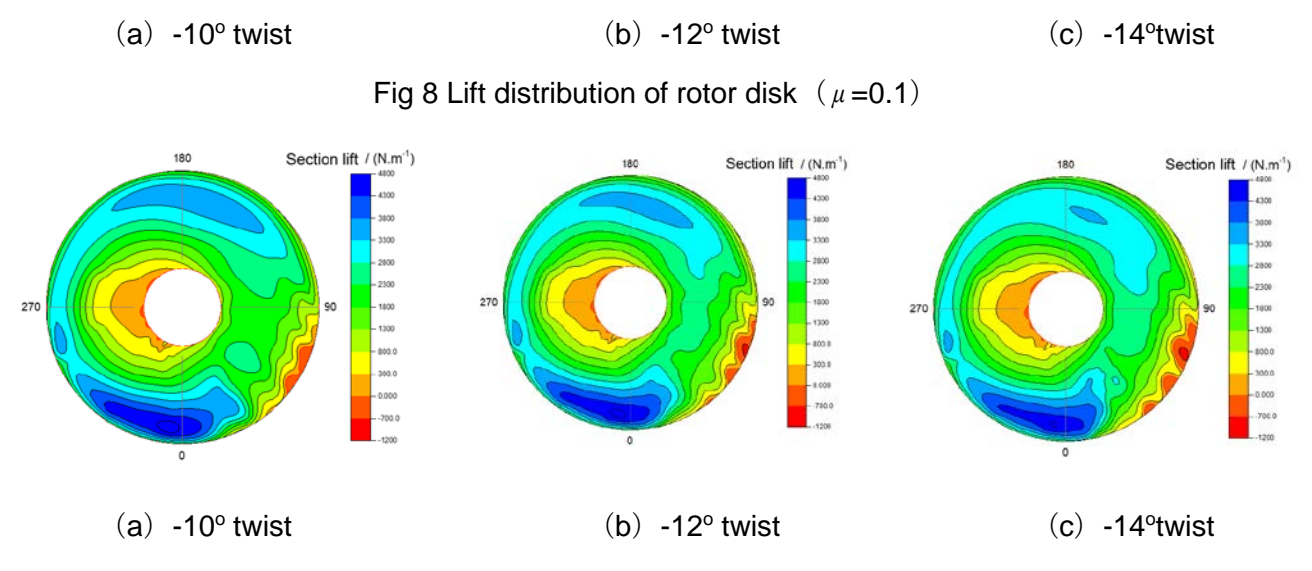


Fig 9 Lift distribution of rotor disk ($\mu = 0.25$)

The result of blade tip flap response in two advance ratios is shown in Fig 10. At $^{\mu}$ =0.1, the blade tip flap displacement exhibited dominance of the first harmonic with small harmonics, indicating a significant effect of blade vortex interaction on blade flap at low speeds. As the negative twist distribution increased, the blade tip flap displacement decreased. In low-speed flight, appropriately increasing negative twist led to a decrease in lift peak value and an increase in rotor efficiency due to reduced higher order harmonics caused by less blade vortex interaction. At $^{\mu}$ =0.25, the blade tip flap response was primarily characterized by second-order harmonics with peak values appearing at 90° and 270° regions. The influence of negative twist was minimal; however, larger negative twists resulted in smaller tip flap displacements in the 90° region due to downward moment caused by negative lift.

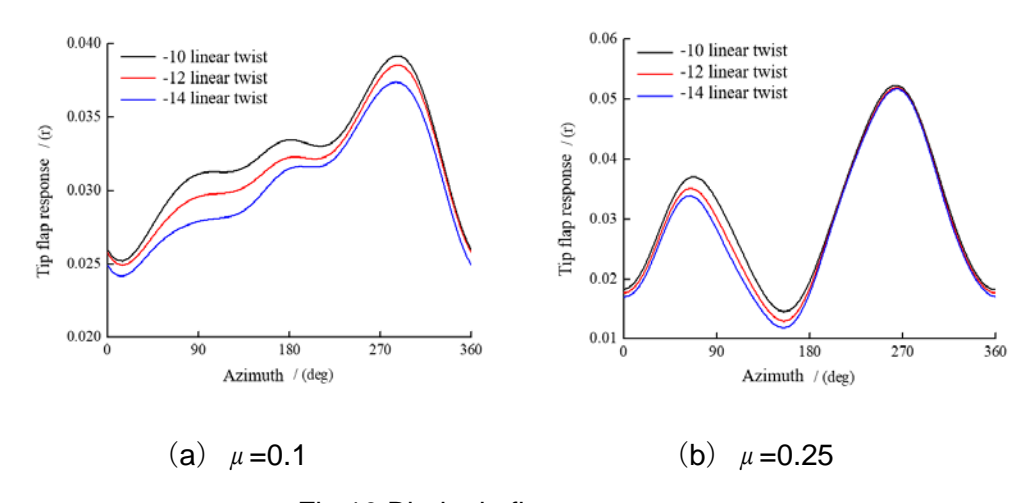


Fig 10 Blade tip flap response

Fig 11 and Fig 12 are the blade root vertical shear force and flap bending moment at a distance of 0.2r section in different flight speed and twist distribution. Bo105 rotor are four blade, so the 3^{rd} to 5^{th} order harmonic loads would transferred to hub. In low speed flight(μ =0.1), the 3^{rd} to 5^{th} order harmonic

blade root vertical shear force and flap bending moment stayed at a high level, which indicated that the blade vortex interaction had an obvious effect to blade aerodynamic loads and structure loads. The vertical shear force and flap bending moment decreased whit the larger linear negative twist, due to larger linear negative twist conducive to decrease the peak value of rotor lift and reduce high-order aerodynamic forces. But excessive increase negative twist angle, the 5th order harmonic blade root vertical shear force and flap bending moment would increase and adverse to vibration. The Fig 11(b) and Fig 12(b) show a sharply increase in the 5th order harmonic.

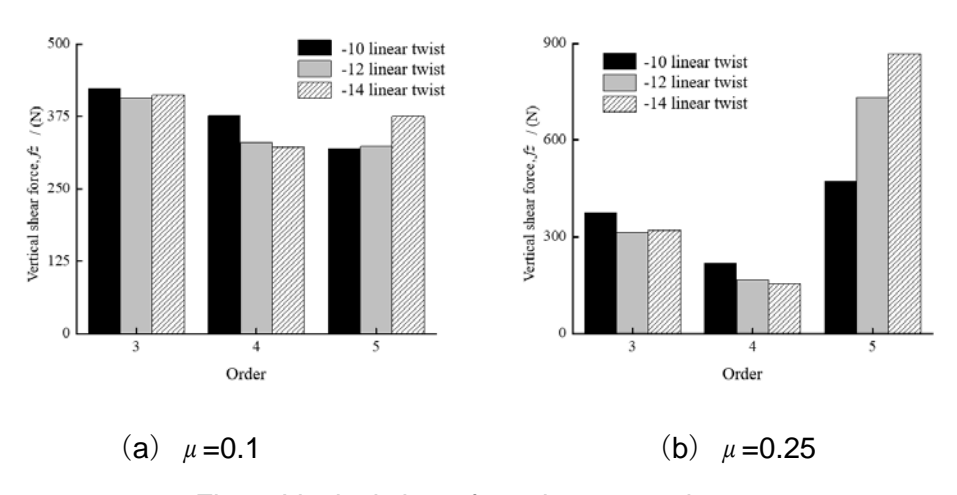


Fig 11 Vertical shear force in 0.2*r* section

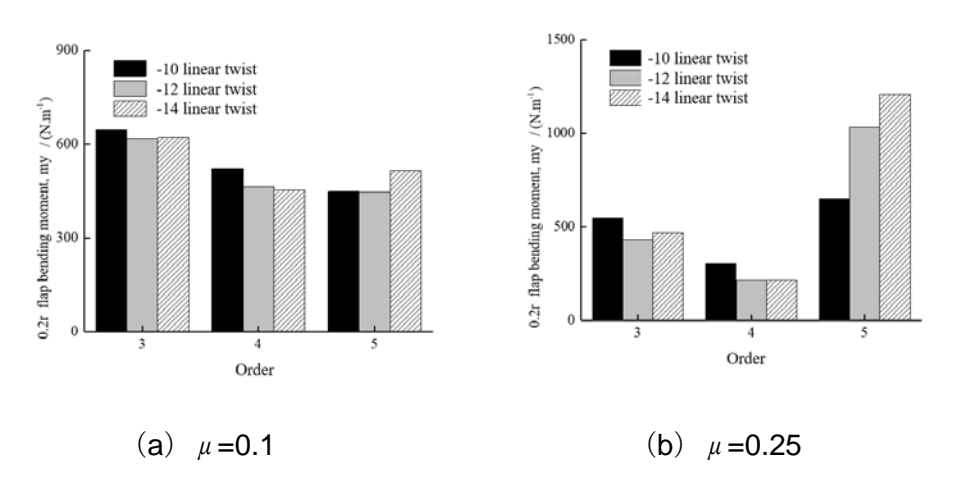


Fig 12 Flap bending moment in 0.2r section

Tab 4 and Tab 5 are the result of the 4th order harmonic hub loads in two flight speed include hub vertical force Fz, hub roll moment Mx, and hub pitch moment My. The hub vertical force was transferred by blade root vertical shear force, so the trend of hub vertical force was the same with the blade root vertical shear force(Fig 11)). The hub roll moment and pitch moment were transferred from the 3rd and 5th order harmonic of blade flap bending moment. The same trends that the larger negative twist, the more serious in vibration loads.

Tab 4 The 4th order harmonic hub loads ($\mu = 0.1$)

| | Fz (N) | Mx (N.m) | My (N.m) |
|-------------------|--------|----------|----------|
| -10° linear twist | 1520 | 2947 | 575 |
| -12° linear twist | 1330 | 2865 | 512 |
| -14° linear twist | 1296 | 3054 | 400 |

Tab 5 The 4th order harmonic hub loads ($\mu = 0.25$)

| | | Fz (N) | Mx (N.m) | My (N.m) |
|------|--------------|--------|----------|----------|
| -100 | linear twist | 539 | 1546 | 2952 |
| -120 | linear twist | 316 | 1822 | 3889 |
| -140 | linear twist | 307 | 2077 | 4494 |

4.2 Different blade tip twist distribution

The variable blade twist design were applied in UH-60A rotor[14] to improve rotor performance and reduce the vibration loads. So three different blade twist design were analyzed base on Bo105 rotor in this part, namely -14° linear twist, 0° twist in 0.95r, 14° twist in 0.95r. In this part, only μ =0.25 condition was analyzed. Fig 13 are lift distribution result. It showed that the region of negative lift at blade tip in advancing side were reduced with blade tip twist angle increased. The lift peak value in 0°, 180° region also decreased, and it was beneficial for rotor performance and vibration.

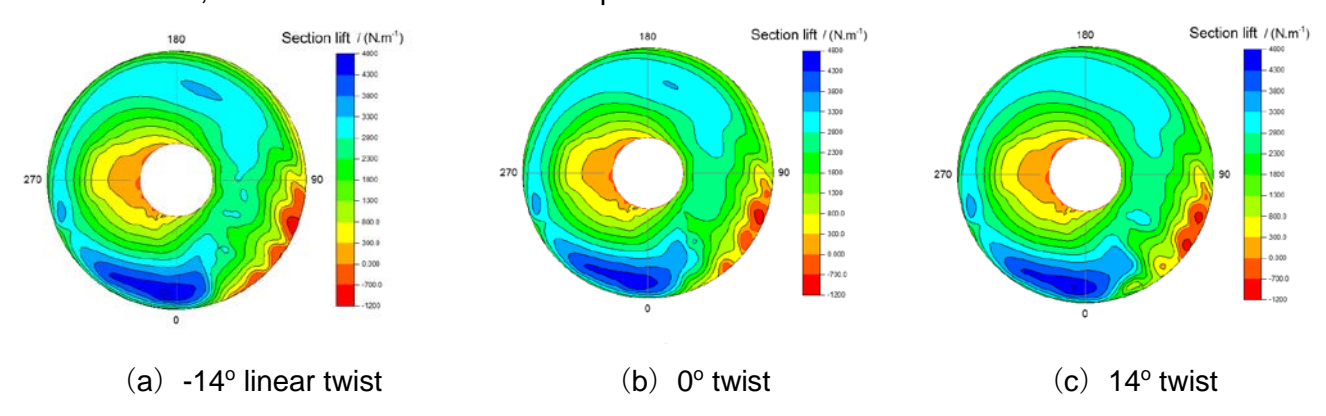


Fig 13 Lift distribution of rotor disk

Fig 14 are blade vertical shear force fz in 0.2r section result. With the blade tip twist angle increased, the 3rd to 5th order harmonic of fz decreased. It was further provided that the blade tip twist angle have strong influence in high order harmonic structure loads. Tab 6 was the result of hub loads. The vertical hub force and roll moment were obviously affected by twist angle. Above all, the result showed that the positive blade tip twist angle would reduce rotor vibration loads in forward flight.

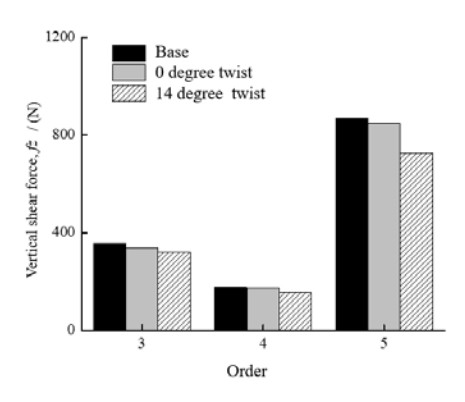


Fig 14 Vertical shear force in 0.2r section

Tab 6 The 4th dynamic loads in rotor hub(μ =0.25)

| | Fz (N) | Mx (N.m) | My (N.m) |
|------------|--------|----------|----------|
| -14° twist | 401 | 2077 | 4494 |
| 0° twist | 362 | 1907 | 4464 |
| 14° twist | 307 | 1578 | 4058 |

4.3 Different blade tip twist distribution at sweep blade

The blade of UH-60A have an obvious sweep angle in blade tip to reduce the tip mach number, and reduce the strength of blade tip vortex. It is a good design for vibration and aero efficiency. The three different sweep angle at 0.95r section were analyzed base on 14° twist angle in this part, namely 0° , 10° , 20° sweep angle. In this part, only μ =0.25 condition was analyzed. Fig 15 showed that the lift have not much change, only small different in 90° region. The result indicated that the sweep angle in blade tip would have small impact base on positive twist in blade tip.

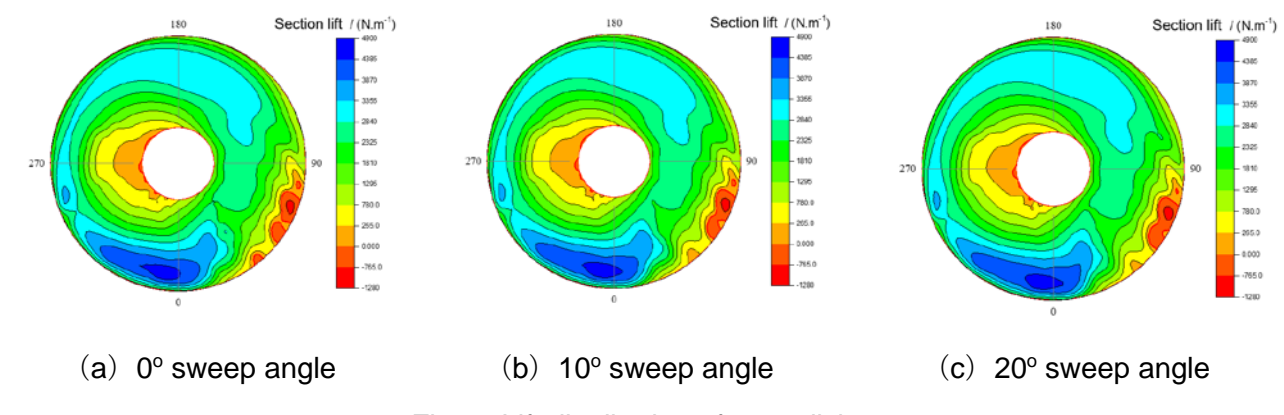


Fig 15 Lift distribution of rotor disk.

5 Conclusion

This paper focuses on the influence of distribution of blade tip torsion on rotor vibration loads. A rotor aeroelastic loads computing model were adopted. The problem of rotor dynamic load variation

caused by different tip twist distribution design was analyzed in detail. The result support the following conclusions:

- (1)In low flight speed, the rotor aerodynamic efficiency would increase with the larger negative twist angle at blade tip, and the blade tip flap response would decrease. But, beyond the medium flight speed, the rotor dynamic loads would increase. The larger negative twist angle would strongly increase the hub roll moment and pitch moment in a hingeless rotor.
- (2)The positive twist angle at blade tip would reduce the rotor dynamic loads beyond the medium flight speed. The sweep angle would have little influence in dynamic loads base on positive twist angle at blade tip.

References

- [1] Ryan P. P, Peretz P. F. Vibration reduction in rotorcraft using closed-loop active flow control[C]// The Vertical Flight Society's 77th Annual Forum & Technology Display, Virtual, Vertical Flight Society, 1356-1371, 2021.
- [2] Hyeonsoo Y, Mark P, Thomas R. Investigation of UH-60A Rotor Structural Loads From Flight and Wind Tunnel Tests[C]//The 72nd American Helicopter Society International Annual Forum. Florida, USA, American Helicopter Society, 1185-1205, 2016.
- [3] Thomas F. Advanced Rotor Blade Design based on High-Fidelity Computational Fluid Dynamics[D]. UK: University of Glasgow, 20-65, 2021.
- [4] ELI B G, KENNETH C H. Minimum loss load, twist, and chord distributions for coaxial helicopter in hover[C]//The 71st American Helicopter Society International Annual. Virginia, USA, American Helicopter Society, 648-657, 2015.
- [5] ELI B G, KENNETH C H. A variational approach to multipoint aerodynamic optimization of conventional and coaxial helicopter rotors[C]//The 71st American Helicopter Society International Annual. Virginia, USA, American Helicopter Society, 752-764, 2015.
- [6] VINCENZO M, GIUSEPPE Q. Optimal tiltrotor blade twist to extend whirl flutter stability boundaries[C]// The Vertical Flight Society's 79th Annual Forum & Technology Display, Virtual, Vertical Flight Society, 985-1001, 2023.
- [7] PAVEL B. Bend-twist coupled carbon-fiber laminate beams: fundamental behavior and applications[D]. USA: University of Washington, 45-78, 2021.
- [8] SALVATORE A, ANTONIO C, ANTONIO V, et al. Aeroacoustic and structural achievements for a morphing blade twist system developed for the Eurpoean project "Shape adaptive blades for rotorcraft efficiency"[C]//The 15th ASME conference on smart materials, Adaptive structres and intelligent systems, Dearborn, USA, 375-389, 2022.
- [9] SHIN S J, CESNIK E S, MATTHEW L W. Dynamic response of active twist rotor blades[J]. Smart Materials and Structures, 10(01): 121-132, 2020.
- [10] AMDEURI S, CONCILIO A, DIMINO I, et al. SMA blade twist system: form the requirements to the demonstration in relevant environment[C]//The Vertical Flight Society's 79th Annual Forum & Technology Display, Virtual, Vertical Flight Society, 1224-1233, 2023.
- [11] SALVATORE A, MONICA C, ANTONIO C, et al. Experimental tests of a SMA based blade twist system: wind tunnel and whirl tower outcomes[C]//The 15th ASME conference on smart materials. Dearborn, USA, Adaptive

- structres and intelligent systems, 487-499, 2022.
- [12] LEE H, Sengupta B, Araghizadeh M S. Review of vortex methods for rotor aerodynamics and wake dynamics[J]. Advances in Aerodynamics, 4(1): 283-303, 2022.
- [13] GUNGJIT B, Inderjit C. University of Maryland Advanced Rotorcraft Code Theory Manual[M]. Maryland: University of Maryland College Park, 585-593, 1994.
- [14] YU Zhihao, ZHOU Yun, HUANG Shuilin, CHENG Yi, et al. Rotor aeroelastic loads characteristic analysis in high speed condition[C]//The 18th National aeroelasticity academic conference, Chengdu, Sichuan. 464-472, 2023.

Copyright Statement

The authors confirm that they, and/or their company or organization, hold copyright on all of the original material included in this paper. The authors also confirm that they have obtained permission, from the copyright holder of any third party material included in this paper, to publish it as part of their paper. The authors confirm that they give permission, or have obtained permission from the copyright holder of this paper, for the publication and distribution of this paper as part of the ICAS proceedings or as individual off-prints from the proceedings.